Modification and Intercalation of Layered Zirconium Phosphates: A solid-state NMR Monitoring.

Vladimir I. Bakhmutov,*,† , Yuwei Kan,‡ Javeed Ahmad Sheikh,‡ Julissa González-Villegas,§ Jorge L. Colón, § and Abraham Clearfield.‡

† Laboratory for Nuclear Magnetic Resonance, Department of Chemistry, Texas A&M University, P.O. Box 30012, College Station, TX 77842-3012, United States

‡ Department of Chemistry, Texas A&M University, P.O. Box 30012, College Station, Texas 77842-3012, United States § Department of Chemistry, P.O. Box. 23346, University of Puerto Rico-Río Piedras Campus, University of Puerto Rico, Río Piedras, P.R. 00931

KEYWORDS zirconium phosphates, intercalation, solid-state NMR, cross polarization

Corresponding Author: Email: bakhmoutov@chem.tamu.edu

Abstract

Several layered zirconium phosphates treated with Zr(IV) ions, modified by monomethoxy-polyethyleneglycol-monophosphate and intercalated with doxorubicin hydrochloride have been studied by solid-state MAS NMR techniques. The organic components of the phosphates have been characterized by the $^{13}C\{^{1}H\}$ CP MAS NMR spectra compared with those of initial compounds. The multinuclear NMR monitoring has provided to establish structure and covalent attachment of organic/inorganic moieties to the surface and interlayer spaces of the phosphates. The MAS NMR experiments

including kinetics of proton-phosphorus cross polarization have resulted in an unusual structure of zirconium phosphate **6** combining decoration of the phosphate surface by polymer units and their partial intercalation into the interlayer space.

Introduction.

During the last decades, extensive studies in the chemistry of layered zirconium phosphate materials (named here and below as ZrP) aimed at modification of their size, morphology and properties[1-7] have resulted in their wide practical applications as biosensors, fuel cells, and catalysts. New properties of ZrP materials can be obtained by intercalation of different species causing an increase in interlayer distances. For example, α-zirconium phosphate (α-ZrP) of formula $Zr(HPO_4)_2 \bullet H_2O$, itself, has a small interlayer distance of 7.6 Å, which limits its applications. However by intercalating organic compounds, such as amines, quaternary ammonium ions[7] or biomolecules[6] the interlayer distance can be increased to allow uptake of different cationic complexes, pillaring agents and many others including creation of molecular systems used for drug delivery.[4-6,8] The applications can be significantly improved by a special design of the zirconium phosphate surface with specific organic/inorganic groups.[9]

Generally, the synthesis of the hybrid zirconium phosphates and intercalated systems leads to products which are difficult to analyze in structural terms because of their amorphous character. Different methods, such as thermogravimetry and X-ray

powder diffraction (XRPD) experiments can characterize such hybrid molecular systems. For example, the XRPD method can show intercalation of various organic/inorganic components into the zirconium phosphate framework. However it is obvious that the XRPD information, illustrating a change in the interlayer distance is not enough for more detailed structural conclusions.

Potentially, valuable data on hybrid materials can be collected by solid-state ^{31}P NMR techniques,[10] allowing determinations of different sites in molecular systems under examination, for example, phosphorus sites.[7, 9, 11, 12] In this work we use solid-state MAS NMR to monitor zirconium phosphate in its alpha phase, α-Zr P (compound **1**), treated with Zr (IV) ions and monomethoxy-polyethyleneglycol-monophosphate (m-PEG-PO_3) leading to materials Zr (IV)/Zr P (compound **2**) and m-PEG-PO_3/Zr (IV)/Zr P (compound **3**), respectively. We also describe MAS NMR spectra and their evolution from **1** to material DOX/Zr P (compound **4**) intercalated with doxorubicin (DOX), treated by Zr (IV) ions (Zr (IV)/DOX/Zr P) (compound **5**) and m-PEG-PO_3 to provide biocompatibility in material m-PEG-PO_3/Zr (IV)/DOX/Zr P (compound **6**). Figure 1 shows stylized structures of desired decorated (A) and intercalated (B) products.

Here Figure 1

The aim of the work is establishment of spectral manifestations corresponding to intercalation and covalent attachments of organic and inorganic species, used for decoration of the zirconium phosphate surface, when amounts of decorating components

are low. In addition a NMR analysis is particularly problematic when the changes in phosphorus chemical shifts expected after modifications of zirconium phosphates are insignificant.

Experimental

The $^{31}P\{^{1}H\}$, $^{13}C\{^{1}H\}$ and ^{1}H MAS NMR experiments were carried out with a Bruker Avance-400 solid-state NMR spectrometer (400 MHz for ^{1}H nuclei) equipped with a standard two-channel 2.5-mm MAS probe head. The standard single pulse (direct nuclear excitation) and/or CP pulse sequences were applied for nuclei ^{31}P and ^{13}C at time delays needed for the full spin-lattice relaxation. The contact times of 2 and 6 ms were adjusted for ^{13}C and ^{31}P nuclei, respectively, to observe the regular proton-carbon and proton-phosphorus cross-polarization (CP) MAS NMR spectra. Due to relatively small amounts of organic components the $^{13}C\{^{1}H\}$ CP MAS NMR experiments have required large numbers of scans (25000 – 27000). The external standards used for ^{1}H, ^{13}C and ^{31}P NMR were TMS and H_3PO_4 solution, respectively.

Kinetics of proton-phosphorus cross polarization has been studied by variations in contact times between 100 and 10000 μs used for the $^{31}P\{^{1}H\}$ CP MAS NMR experiments. The kinetic data have been treated with a standard fitting computer procedure.

Initial zirconium phosphate α-ZrP has been obtained according to[13] by dehydration of θ-ZrP, obtained by the direct synthesis method reported by Kijima.[14] The details of the synthesis and procedures on treatments of **1** by Zr(IV) ions, m-PEG-PO_3 and DOX are being published separately. A brief summary of the XRPD data is presented here. The XRPD patterns obtained by the experiments performed from 2 to 40° (2θ-angle) with a Bruker-AXS D8 short arm diffractometer equipped with a multi-wire lynx eye detector using Cu Kα radiation (λ = 1.542 Å) and operated at a potential of 40 kV and a current of 40 mA, show peaks corresponding to a d-spacing of 7.6 Å for compounds **1**, **2** and **3** and 20.3 Å for compounds **4**, **5** and **6**.

Results and Discussion

*Modification of the phosphate surface by Zr(IV) ions: materials **1** and **2**.* The $^{31}P\{^{1}H\}$ CP and $^{31}P\{^{1}H\}$ MAS NMR NMR spectra of **1** show a major resonance at δ of -19.1 ppm and two weak resonances at δ of -17.3 and -20.8 ppm in full accordance with the data reported earlier.[9, 11, 12] The dominant signal at -19.1 belongs to HPO_4^{2-} orthophosphate groups in $Zr(HPO_4)_2 \bullet H_2O$. Since ^{31}P resonances in zirconium phosphates experience high-field displacements from -16.6 to -21.7 ppm with decreasing amounts of crystallization water,[7, 11] the weak resonances at δ of -17.3 ppm and -20.8 ppm can be

assigned to HPO_4^{2-} orthophosphate groups located in more and less hydrated areas of the ZrP material, respectively.

Here Figure 2

Figure 2A shows the $^{31}P\{^1H\}$ CP MAS NMR spectrum of **2** similar to that of **1**: again, three phosphorus resonances are observed at cross polarization. Proton-phosphorus cross polarization in ^{31}P NMR of zirconium phosphates is known to occur via closest protons of HPO_4^{2-} groups and water protons, forming a hydrogen bond network in the surface and interlayer space of the phosphates.[7, 12] Therefore, the high-field resonance at δ of – 21.7 ppm increased in the $^{31}P\{^1H\}$ MAS NMR spectrum of **2** (Figure 2A) is consistent with its assignment to the less hydrated area, where cross polarization is less effective. The extended reflux of **1** at the treatment with Zr(IV) ions can cause some of the interlayer water to escape the interlayer space.

A weak wide resonance, appearing between – 27 and - 28 ppm in the $^{31}P\{^1H\}$ MAS NMR spectrum of **2** (Figure 2A) is an most important spectral feature typical of all the materials after their Zr(IV) treatments. According to ^{31}P chemical shifts reported for zirconium phosphates,[11, 12, 15, 16] this line definitely belongs to PO_4^{3-} groups coordinated with Zr(IV) ions. Since the treatment of **1** by Zr(IV) ions does not expand the interlayer distance (7.6 Å), the PO_4^{3-} groups coordinated with Zr(IV) ions are most likely located in the surface of **2**. This surface is generally amorphous and therefore the PO_4^{3-} resonance is broad. A deconvolution of the signals in the $^{31}P\{^1H\}$ MAS NMR spectrum of **2** gives a

HPO_4^{-2} / PO_4^{-3} ratio of (23-20) / 1. This ratio is quite reasonable at locations of M(IV) ions in the phosphate surface.[17, 18]

*Modification of the ZrP phosphate surface by m-PEG-PO_3 polymer: compound **3***. The $^{13}C\{^1H\}$ CP MAS NMR spectrum of **3** exhibits a (O-CH_2-CH_2-O) singlet at δ of 71.0 ppm close to the resonance at 70.8 ppm observed in the $^{13}C\{^1H\}$ CP MAS NMR spectrum of initial m-PEG-PO_3. At the same time, no ^{31}P signal at δ of -1 ppm of initial polymer m-PEG-PO_3 is observed in the $^{31}P\{^1H\}$ MAS NMR spectrum of **3** even at long-term accumulation. Since after the m-PEG-PO_3 treatment the interlayer distance in **3** does not change (7.6 Å), polymer molecules of the PEG are presumably binding to Zr(IV) ions on the phosphate surface with the bonding mode in Figure 3 earlier suggested

Here Figure 3

for other M(IV) ions.[17, 18] In fact, intercalation of polymers in ZrP materials[19, 20] is generally accompanied by larger interlayer distances.

A ^{31}P NMR identification of the (Zr-O)$_3$-***P***-OCH_2- phosphorus sites, shown in Figure 3 is difficult. First, for example, the ***P***-O-C linkage in decorated material 1,2-epoxyoctadecane/ZrP gives the ^{31}P peak at -22.4 ppm,[9] i.e. in a zone of ^{31}P chemical shifts already occupied by other resonances of **3** in Figure 2. Second, the intensity of a P-OCH_2 signal expected for the structure in Figure 3 will be nine-times smaller than that of the weak broad resonance belonging to PO_4^{3-} groups coordinated with Zr(IV) ions (δ = – 27 ÷ - 28 ppm in Figure 2).

The $^{31}P\{^{1}H\}$ CP MAS NMR spectra of **3** and **2** in Figure 2A are practically identical. Thus, the presence of $(CH_2\text{-}CH_2\text{-}O)_n$- protons in the m-PEG-$PO_3$ polymer chains does not affect the proton-phosphorus cross polarization in the phosphate framework. This is not surprising if distances between the protons of polymer chains and ^{31}P nuclei are large (Figure 3). The situation changes in the $^{31}P\{^{1}H\}$ MAS NMR spectra obtained by direct ^{31}P excitation. Here the resonance of **3** at δ of -21 ppm looks more intense than that in the spectrum of **2** (Figure 2A). To estimate this increase semi-quantitatively, the $^{31}P\{^{1}H\}$ MAS NMR spectra of both compounds **2** and **3** have been scaled to provide the same intensity of the broad signals at δ of – 28 ppm. Then, a weak signal at δ of -22.7 ppm can be obtained by subtraction of one spectrum from the other one as shown in Figure 2B. This signal can definitely be assigned to $(Zr\text{-}O)_3$-***P***-$O(CH_2)$ fragments in the phosphate surface of **3** (Figure 3). A Zr-***P***-O-Zr/$(ZrO)_3$-***P***-OCH_2 ratio is determined as ~5-6 / 1 which is close to 9 / 1 expected for the structure in Figure 3. In fact, the above procedure is not accurate. Thus the solid-state NMR data supports well the desired structure in Figure 1A.

*Intercalation of DOX: compound **4**.* The reaction of DOX with θ-ZrP at the DOX : ZrP molar ratio of 1:5 resulted in material **4** having an expanded interlayer distance of 20.3 Å. Figure 4 shows the $^{13}C\{^{1}H\}$ CP MAS NMR spectrum of initial compound DOX.

Here Figure 4 and 5

The number of the relatively narrow resonances and their chemical shifts are very similar to those reported for a water solution of DOX,[21] where all of the lines have been well assigned. Based on the solution NMR, the assignments of the signals are (see Figure 5): 213.8 ppm (C(13)), 187.1 ppm (C(5,12)), 161.3 ppm (C(1)), 156.6 ppm (C(6)), 154.5 (C(11)), 135.0 ppm (C(3)), 119.1 (C(2)), 116.3 ppm (C(4)), 99.6 ppm (C(1')), 77.9 ppm (C(8)), 68.1 ppm (C(10)), 56.8 ppm (CH_3O), 48.9 ppm (C(3')), 35.8 ppm (C(9) and C(7)), 30.2 ppm (C(2')) and 19.3 ppm (CH_3). The resonances at δ of 136.6, 133.3, 127.3, 121.9, 113.2 and 111.2 ppm obviously belong to key–carbons of the aromatic rings. Finally the signals of carbons C(4',5') and C(14), observed in solutions are not resolved in the solid state because of line overlaps.

The $^{13}C\{^1H\}$ CP MAS NMR spectra of material **4** and initial DOX are compared in Figure 4. The resonances of intercalated DOX molecules are strongly broadened and some of them experience displacements. However, these displacements are small (≤ 2 ppm) and they do not allow to suggest specific interactions between DOX molecules and HPO_4^{-2} phosphate groups, for example H-bonding.[15] One can think that the van der Waals forces are a stabilizing factor of the intercalation. The strongly broadened lines of DOX resonances in **4** are presumably caused by non-uniform molecular orientations of DOX in the interlayer space.

The $^{31}P\{^1H\}$ and $^{31}P\{^1H\}$ CP MAS NMR spectra of material **4** are shown in Figure 6. It is remarkable that the $^{31}P\{^1H\}$ CP MAS NMR spectrum of **4**, on the whole, is

Here Figure 6

similar to that of **1**:[9, 11, 12] three HPO_4^{2-} resonances are observed at δ of -17.6, -19.3, and -21.4 ppm. However the high-field resonance of **4** is more intense probably due to cross polarization occurring via protons of intercalated DOX molecules in addition to water protons. A more significant enhancement of this high-field resonance is observed in the $^{31}P\{^1H\}$ MAS NMR spectrum of compound **4**. This fact provides to assume that the less hydrated area develops due to intercalated DOX molecules that displace water molecules from the interlayer space in accordance with the structure in Figure 7.

Here Figure 7

*Modification of the phosphate surface of **4**: compounds **5** and **6***. The ^{13}C MAS NMR monitoring of a material obtained after the treatment of **4** with Zr(IV) ions shows that chemical shifts of the ^{13}C DOX resonances do not change from material **4** to material **5**. However, the resonance intensities in **5** are significantly reduced relatively to those in the $^{13}C\{^1H\}$ CP MAS NMR spectrum of **4** obtained at the same number of scans. Although this decrease is difficult to estimate quantitatively by ^{13}C CP NMR, it shows that ca. a half of DOX molecules leaves the interlayer space after the treatment of **4** with Zr(IV) ions. It is interesting that the interlayer distance in 5 remains the same (20.3 Å).

It is remarkable that the $^{31}P\{^1H\}$ CP MAS NMR spectrum of **5** in Figure 6 is now more similar to that of **1**. Indeed, the intensity of the signal at -21.4 ppm decreases relatively to that of the same resonance in **4**. This effect agrees well with a partial

elimination of DOX molecules. As in the case of **2**, the $^{31}P\{^{1}H\}$ MAS NMR spectrum of **5** exhibits a weak resonance between – 27 and- 28 ppm belonging to PO_4^{3-} groups coordinated with Zr ions in the phosphate surface. Thus, the structure of **5** is close to that in Figure 7.

The treatment of **5** with polymer m-PEG-PO_3 leads to phosphate **6** having the same interlayer distance of 20.3 Å. As earlier, the ^{31}P signal at δ of -1 ppm corresponding to initial m-PEG-PO_3 is not detected in the $^{31}P\{^{1}H\}$ MAS NMR spectrum of **6** while $(CH_2\text{-}CH_2\text{-}O)_n$- groups are observed in the $^{13}C\{^{1}H\}$ CP MAS NMR spectrum in Figure 8 as two resonances

Here Figure 8

at 70.6 and 67.3 ppm discussed below. In addition, $(CH_2\text{-}CH_2\text{-}O)_n$- groups appear in the ^{1}H NMR spectrum of **6** as a very intense line at δ of 3.9 ppm. In contrast, the intensity of the $(CH_2\text{-}CH_2\text{-}O)_n$- groups in the $^{13}C\{^{1}H\}$ CP MAS NMR spectrum of **6** is as low as that of the C(10) resonance in DOX (Figure 8). It is not surprising because all of the $^{13}C\{^{1}H\}$ CP MAS NMR spectra in this work have been obtained with the standard contact time of 2000 μs while an effective cross-polarization in individual m-PEG-PO_3 requires much less contact times of 300 μs.[22]

The $^{31}P\{^{1}H\}$ MAS NMR spectrum of **6** in Figure 6 obtained at ^{31}P direct excitation is similar to those of DOX-intercalated compounds **4** and **5**. It shows the most intense resonance at -22 ppm and the weak wide resonance between -27 and - 28 ppm for

(PO_4^{3-}) groups. The latter does not change in the absence of {^{1}H} –decoupling, while the other resonances experience remarkable broadenings to support the signal assignments carried out above. In contrast, the ^{31}P{^{1}H} CP MAS NMR spectrum of **6** deserves special attention. As seen, the intense resonance centered at δ of -22.6 ppm is generated by the proton-phosphorus cross polarization. Non is observed in the ^{31}P{^{1}H} CP MAS NMR spectrum of compound **3**, emphasizing, thus, the principal difference between these two materials. The appearance of a new proton continuum in material **6**, corresponding to the effective proton-phosphorus cross polarization, can be connected with a feature of polymer $(Zr\text{-}O)_3\text{-}P\text{-}O\text{-}CH_2$- units, where two sorts of $(CH_2\text{-}CH_2\text{-}O)_n$- chains, "out" and "in" in Figure 9, will have different environments. The ^{13}C{^{1}H} CP MAS NMR spectrum

Here Figure 9

of **6** in Figure 8 supports well this suggestion: two $(CH_2\text{-}CH_2\text{-}O)_n$- resonances at 70.6 and 67.3 ppm are observed versus the singlet at δ of 71.0 ppm in the ^{13}C{^{1}H} CP MAS NMR spectrum of **3**. A partial intercalation of PEG molecules can be caused by the initial treatment of **4** by Zr(IV) ions, when a part of DOX molecules leaves the interlayer space.

To rationalize the nature of the cross polarization in material **6**, the experiments on the CP kinetics[23-25] have been performed by variation in cross-polarization contact time between 100 and 10000 μs. Potentially the kinetic data in Figure 10 can result in

Here Figure 10

determination of the cross-polarization constants T_{H-P} and ^1H relaxation times $T_1\rho(H)$ in the rotating framework. These parameters, particularly, the ^1H $T_1\rho(H)$ relaxation times, characterize the protons in material **6**, providing the cross polarization process.

The experimental CP curves in Figure 10 have been treated for the resonances at -19.4 and -22.6 ppm in the framework of a classical spin I-S model[23] valid for weak heteronuclear dipolar interactions, when the cross-polarization occurs via remote protons. Equation (1) has been applied for fitting procedures, where I(t), T_{H-P}, $T_1\rho$ (H) and t are the signal intensity, the cross polarization constant, proton relaxation time, and contact time,

$$I(t) = I_0(1 - T_{H-P}/T_1\rho(H))^{-1}(\exp(-t/T_1\rho(H)) - \exp(-t/T_{H-P})) \quad (1)$$

respectively. Good fittings obtained for both ^{31}P resonances in Figure 10 demonstrate the validity of the above model. As seen, the CP behavior of these resonances in material **6** is completely different.

The CP kinetics for the signal at -19.4 ppm gives values of T_{H-P} and ^1H $T_{1\rho}(H)$ calculated as 1.3 and 27 ms, respectively. Very similar values have been obtained for the ^{31}P resonances of compound **5**: T_{H-P} = 1.4 ms and ^1H $T_{1\rho}(H)$ = 30 ms. In contrast, the resonance at -22.6 ppm of the polymer-containing compound **6** shows a strongly shorter the $T_{1\rho}(H)$ relaxation time of 5 ms at the same T_{H-P} constant (1.3 ms).

In general, interpretation of T_{H-P} constants is not trivial because they depend on internuclear H-P distances via the $1/r^3$ factor, the number of protons around ^{31}P nuclei,

and the mobility groups under investigation. [23] In other words, the larger number of neighboring protons can be compensated by an increase in P-H distances or group mobility. For example, groups HPO_4^{-2} in phosphate **1** ($Zr(HPO_4)_2 \bullet H_2O$) show the constant T_{H-P} of 0.85 ms.[12] This time is remarkably shorter than 1.3 and 1.4 ms, found for the modified zirconium phosphates having the same groups. In this context, one extra H_2O molecule in γ-$ZrP \bullet 2H_2O$ leads to an unjustifiably-short constant T_{H-P} (HPO_4^{-2}) of 0.15 ms [12] versus compound **1**. Therefore, the most reliable factor affecting the CP kinetics in Figure 10 is the strongly different ^1H $T_1\rho(H)$ times determined for the signals at -19.4 (27 ms) and -22.6 ppm (5 ms) in **6**. These times show two distinguished proton reservoirs leading to the cross polarization. Such reservoirs can be represented by protons HPO_4^{-2} / H_2O (and even DOX) on one hand and protons of $(CH_2\text{-}CH_2\text{-}O)_n$- groups in the polymer chains of PEG on the other hand. The later is well supported by the short ^1H $T_1\rho(H)$ times (0.4 - 8 ms) measured for individual PEG(6000) and its co-crystals with small molecules.[26] Since the relative intensities of three ^{31}P resonances do not change in the $^{31}P\{^1H\}$ CP NMR spectra of **3** with variation in contact time, the location and mobility of m-PEG-PO_3 polymer chains in **3** and **6** are principally different.

The chemistry of layered zirconium phosphates shows that polymer molecules, such as polyethylene[19] or polyetheramine[20] can be intercalated into the interlayer space. Generally increasing the interlayer distance depends on the nature and molecular weights of the polymers. For example, the intercalated polyethylene increases the distance from

24 to 30 Å, while polyetheramines require the interlayer distance of ca. ~ 40 Å to 88 Å at increased molecular weight from 300 to 1000 units.[20] At the same time, if m-PEG-PO_3 polymer or its relatives are arranged within the interlayer space with their chain axis parallel to the layers in α- and γ- zirconium phosphates, the interlayer distances remain between 10 and 22 Å.[27,28] This fact combined with the new channel for the proton-phosphorus cross polarization in **6** via m-PEG-PO_3 protons leads to the structures in Figure 9, where a part of the m-PEG-PO_3 molecules is intercalated in parallel to the layers (structure A). The m-PEG-PO_3 chains can also be intercalated by "creeping" in the interlayer space as shown I structure B. Due to the intercalation, the molecular orientation of PEG moieties, stabilized by van der Waals forces provides the proximity of phosphorous and hydrogen atoms. In this context, the low-frequency mobility of $(CH_2\text{-}CH_2\text{-}O)_n$- groups in m-PEG-$PO_3$ can be actually changed from **3** to **6** leading to the short $T_1\rho(H)$ time of 5 ms in material **6**.

Thus the NMR monitoring shows that the desired structure in Figure 1B preferable in the context of drug delivery is not formed due to a partial intercalation of PEG molecules.

Conclusions

Solid-state multinuclear NMR has been applied for characterization of layered α-ZrP phosphates treated with Zr(IV) ions, modified by monomethoxy-polyethyleneglycol-

monophosphate (m-PEG-PO_3) and intercalated with doxorubicin (DOX) important in the context of drug delivery systems.

All the zirconium phosphates treated with Zr(IV) ions show the ^{31}P resonance at δ of -27 ÷ -28 ppm belonging to the surface phosphorus sites binding to Zr(IV) ions. PEG molecules binding to the phosphate surface show $(ZrO)_3$***P***-(OCH_2)- moieties as a very weak signal at -22.5 ppm in the $^{31}P\{^1H\}$ MAS NMR spectra. The ^{31}P and ^{13}C MAS NMR spectra identify the structure of material **3** where monomethoxy-polyethyleneglycol-monophosphate molecules are attached to Zr(IV) ions on the phosphate surface.

The ^{31}P and ^{13}C MAS NMR experiments including kinetics of proton-phosphorus cross polarization have resulted in an expected structure of the DOX intercalated phosphate **6** combining decoration of the zirconium phosphate surface by polymer units and their intercalation into the interlayer space. Intercalation of m-PEG-PO_3 provides the proximity of $(CH_2\text{-}CH_2\text{-}O)_n$- protons and phosphorus sites giving rise to the additional proton-phosphorous cross polarization mechanism. Formation of this structure is caused by the initial treatment of **4** with Zr(IV) ions, when a part of DOX molecules leaves the interlayer space.

Acknowledgements

This work was supported by the Robert A. Welch Foundation Grant A-0673 (Metal Phosphonates as Crystal Engineered Solids and platforms for drug delivery) and the

Nuclear Energy University Program (DOE) Grant Award #: DE-NE0000746 (Mixed Metal Phosphonate-Phosphate Resins for Separation of Lanthanides from Actinides) , for which grateful acknowledgement is made. We would like to acknowledge the X-ray Diffraction Laboratory at Texas A&M University for the use of the XRPD facilities. JGV acknowledges helpful discussions with Agustín Díaz and partial support by the Puerto Rico-Louis Stokes Alliance for Minority Participation Bridge-to-the-Doctorate Program, NSF Grant Award #1139888.

References

[1] H. Nathan, B. Akhilesh, V. K. Challa, Layered -Zirconium Phosphates and Phosphonates. In *Handbook of Layered Materials*, CRC Press: **2004**

[2] C. Ferragina, R. Di Rocco, P. Giannoccaro, P. Patrono, L. Petrilli, *J. Incl. Phenom. Macro.* **2009,** *63*, 1-9

[3] M. E. B.Santiago, M. M.Vélez, S. Borrero, A. Díaz, C. A. Casillas, C. Hofmann, A. R. Guadalupe, J. L. Colón, *Electroanalysis* **2006,** *18*, 559-572

[4] A. Díaz, V. Saxena, J. Gonzalez,. A. David, B. Casanas, C. Carpenter, J. D. Batteas, J. L. Colón,. A. Clearfield; M. Delwar Hussain, *Chem. Commun.* **2012,** *48*, 1754-1756

[5] A. Díaz, M. L. Gonzalez, R. J. Pérez, A. David, A. Mukherjee, A. Baez, A. Clearfield, J. L. Colón, *Nanoscale* **2013,** *5*, 11456-11463

[6] A. Díaz, A. David; R. Pérez, M. L. González, A. Báez, S. E. Wark, P. Zhang, A. Clearfield, J. L. Colón, *Biomacromolecules* **2010,** *11*, 2465-2470

[7] H. Nakayama, *Phosphorus Research Bulletin* **2009,** *23*, 1-9

[8] J. L. Colón, B. Casañas, Drug Carriers Based on Zirconium Phosphate Nanoparticles. In *Tailored Organic-Inorganic Materials*, John Wiley & Sons, Inc: **2015**; pp 395-437.

[9] B. M. Mosby, A. Díaz, V. Bakhmutov, A. Clearfield, *ACS Appl. Mater. Interfaces* **2014,** *6*, 585-592.

[10] A. Lesage, *Phys. Chem. Chem. Phys.* **2009**, *11*, 6876.

[11] K.-I.Segawa, Y. Nakajima,; S.-I. Nakata, S. Asaoka, H. Takahashi, *J. Catal.* **1986,** *101*, 81-89

[12] N. J. Clayden, *Dalton Trans.* **1987**, 1877-1881

[13] A. Clearfield, A. L. Landis, A. S. Medina, J. M. Troup, *J. Inorg. Nucl. Chem.* **1973,** *35*, 1099-1108

[13] T. Kijima, *Bull. Chem. Soc. Jpn.* **1982,** *55*, 3031-3032

[15] M. Kim, M. Kobayashi, H. Kato, M. Kakihana, *Opt. Photonics J.* **2013,** *3*, 13-18

[16] X. Kong, Characterization of Proton Exchange Membrane Materials for Fuel Cells by Solid State NMR. *PhD Thesis, Iowa State University* **2010**, 11912

[17] B. M. Mosby, M. Goloby, A. Díaz, V. Bakhmutov, A. Clearfield, *Langmuir* **2014,** *30*, 2513-2521

[18] A. Díaz, B. M. Mosby, V. I. Bakhmutov, A. Martí, J. D. Batteas, A. Clearfield, *Chem. Mater.* **2013,** *25*, 723-728

[19] M. Casciola, D. Capitani, A. Donnadio, G. Munari, M. Pica, *Inorg. Chem.* **2010,** *49*, 3329-3336

[20] N. Bestaoui, N. A. Spurr, A. Clearfield, *J. Mater. Chem.* **2006,** *16*, 759-764

[21] A. Vigevani, M. J. Williamson, Doxorubicin. In *Analytical Profiles of Drug Substances*, Klaus, F., Ed. Academic Press: **1981**; Vol. Volume 9, pp 245-274

[22] M. Bardet, G. Gerbaud, Q.-K. Trân, S. Hediger, *J. Archaeol. Sci.* **2007,** *34*, 1670-1676

[23] W. Kolodziejski, J. Klinowski, *Chem. Rev.* **2002,** *102*, 613-628

[24] E. V. Bakhmutova-Albert,; N. Bestaoui, V. I. Bakhmutov, A. Clearfield,; A. V. Rodriguez, R. Llavona, *Inorg. Chem.* **2004,** *43*, 1264-1272

[25] R. Mathew, P. N. Gunawidjaja, I. Izquierdo-Barba, K. Jansson, A. García, D. Arcos, M. Vallet-Regí, M. Edén, *J. Phys. Chem. C* **2011,** *115*, 20572-20582

[26] Z. Zhong, C. Guo, L. Chen, J. Xu, Y. Huang, *Chem. Commun.* **2014,** *50*, 6375-6378

[27] U. Costantino, F. Marmottini, *Mater. Chem. Phys.* **1993,** *35*, 193-198

[28] L. Xiang, Preparation of Layered Intercalation Compounds via One-Pot in SituSynthesis. *Master Degree Thesis. Texas State University-San Marcos*, **2012**.

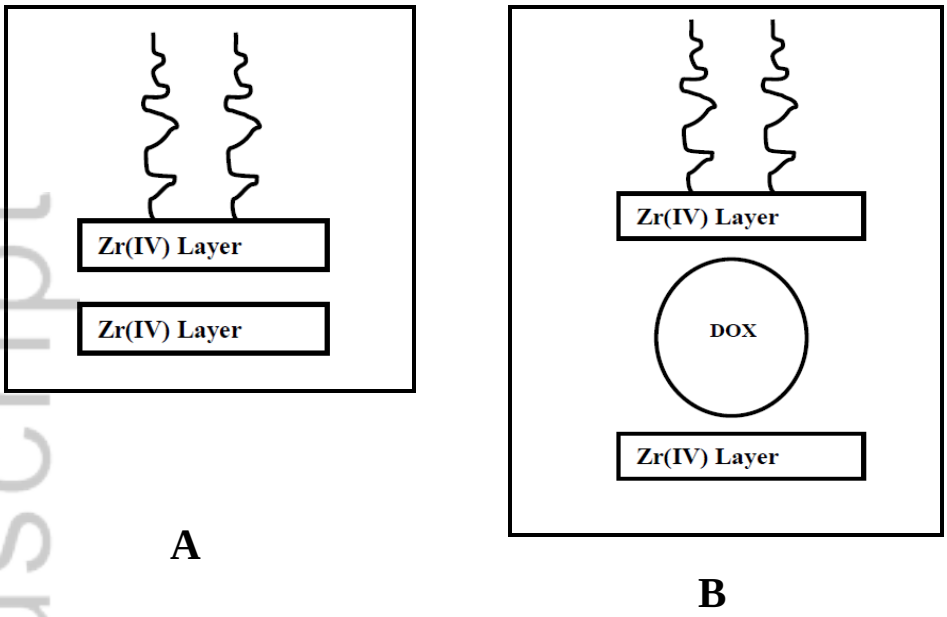

Figure 1. Fragments in stylized structures of desired decorated (A) and intercalated (B) products.

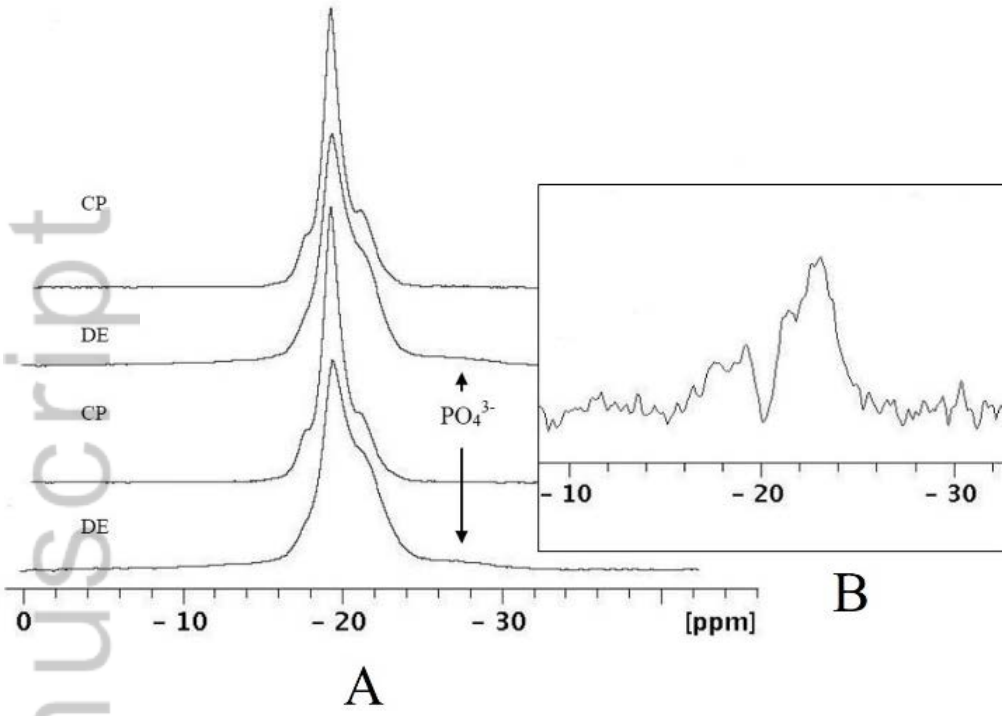

Figure 2. A: $^{31}P\{^{1}H\}$ MAS NMR spectra (6 kHz) (from top to bottom) obtained with cross polorization (CP) and direct excitation (DE) for **2** and **3**; B: a difference ^{31}P NMR spectrum (see the text).

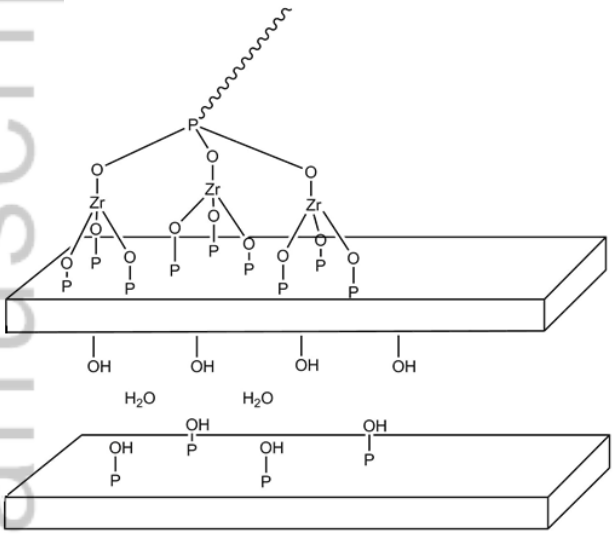

Figure 3. A fragment of an idealized structure for compound **3** with the surface modification by m-PEG-PO_3 polymer units.

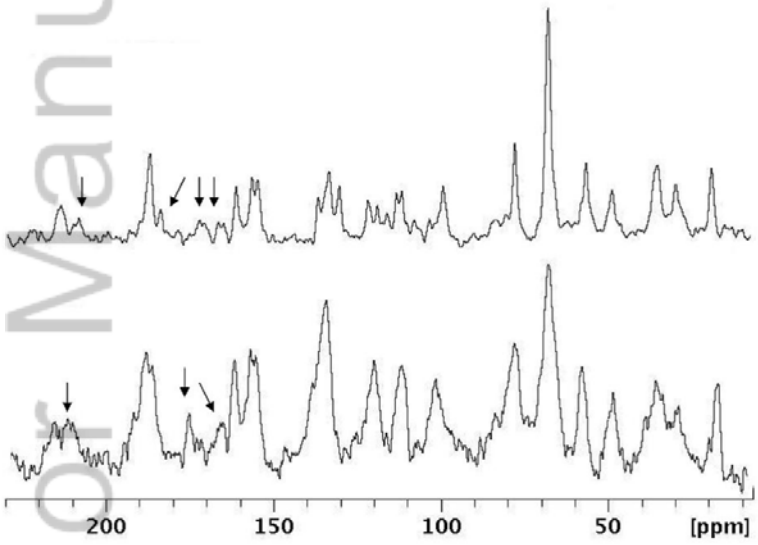

Figure 4. The $^{13}C\{^{1}H\}$ CP MAS NMR spectra of initial DOX (bottom, 6 kHz) and material **4** (top, 5.3 kHz) (the arrows show spinning sidebands).

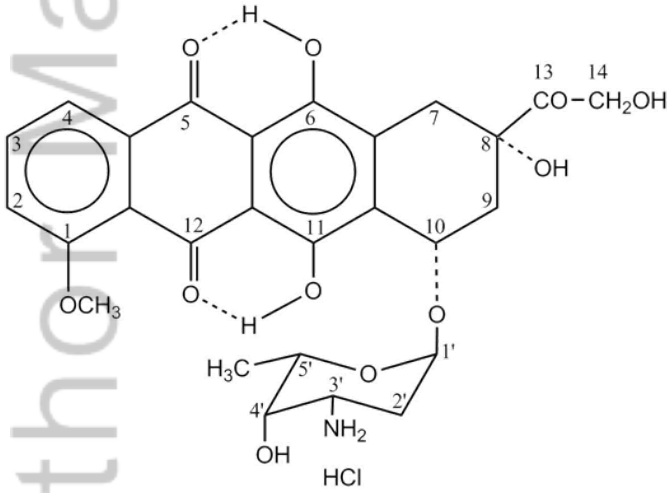

Figure 5. Structure of doxorubicin hydrochloride (DOX).

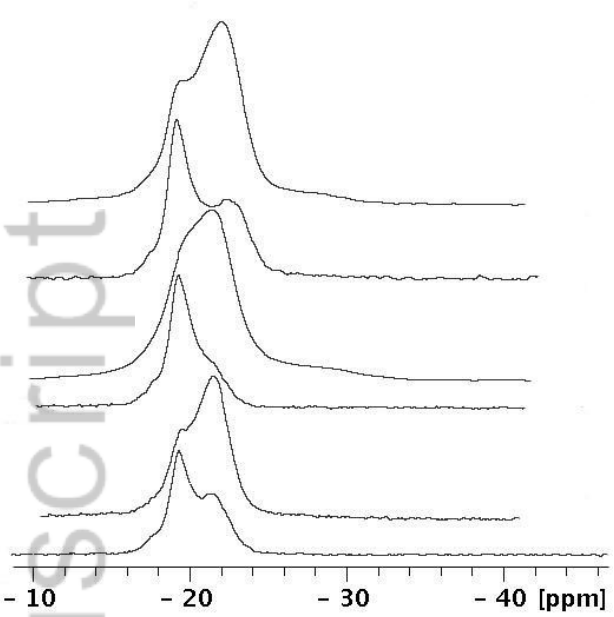

Figure 6. The $^{31}P\{^{1}H\}$ MAS NMR spectra at a 6 kHz spinning rate (from top to bottom), obtained with direct excitation (top) and cross polarization (bottom) for compound **6**; for compound **5**; and for compound **4**.

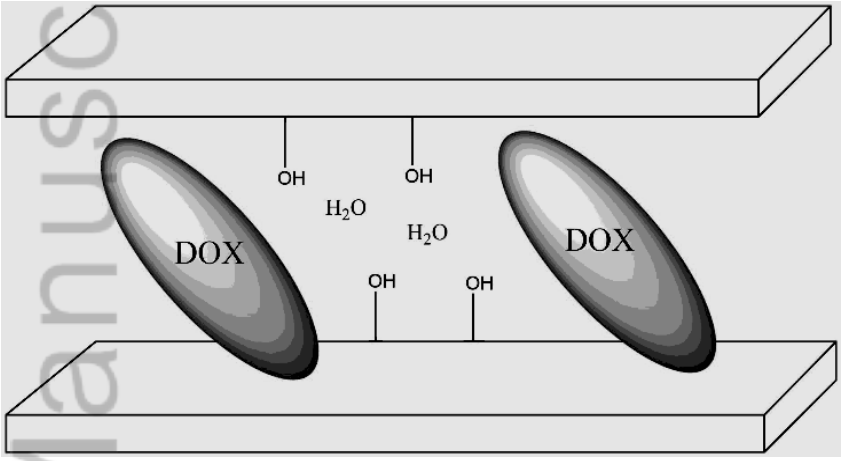

Figure 7. Fragment of idealized structure for compound **4**.

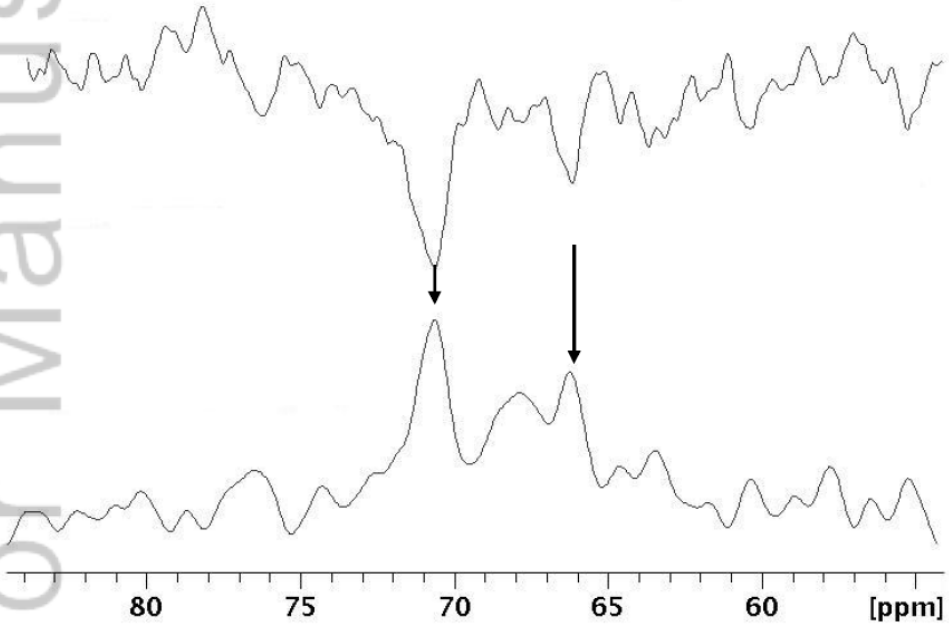

Figure 8. Bottom: the $^{13}C\{^{1}H\}$ CP MAS NMR spectrum of compound **6** shown between 50 and 80 ppm (bottom); top: the difference obtained by subtraction of the ^{13}C $^{13}C\{^{1}H\}$ CP MAS NMR spectra of **5** and **6**.

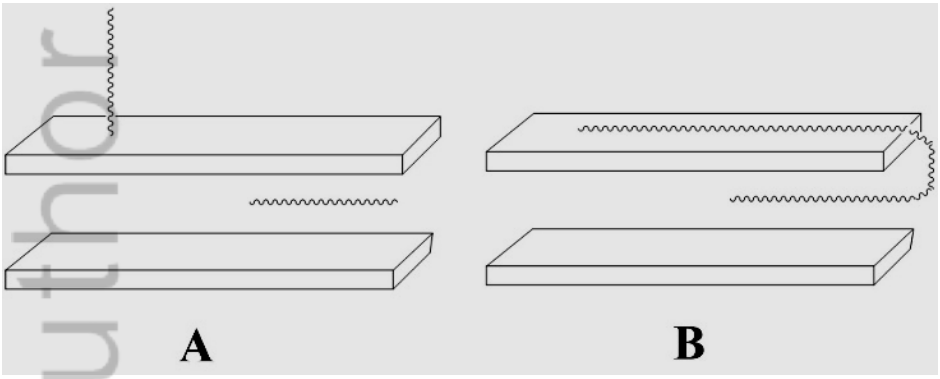

Figure 9. Possible arrangements of a intercalated m-PEG-PO_3 polymer (in addition to a surface polymer) with chain axis parallel to zirconium phosphate layers. The PEG is binding to Zr(IV) ions on the phosphate surface and in the interlayer space. DOX molecules are not shown.

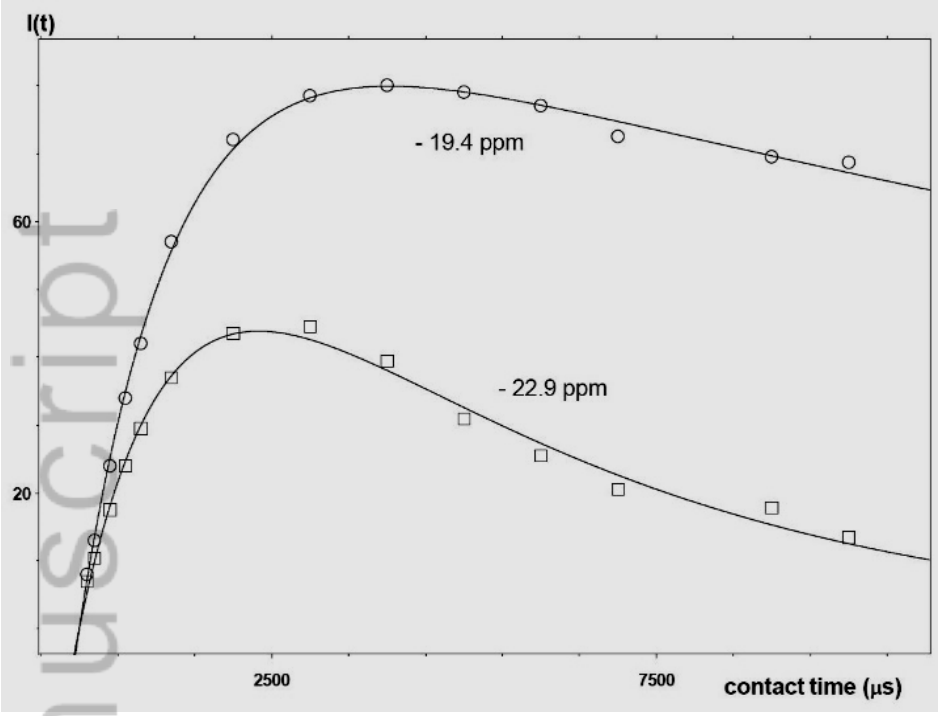

Figure 10. Kinetic curves of proton-phosphorus cross polarization obtained for two phosphorus resonances in material **6**. The data represented in the ^{31}P signal intensity (au) versus contact time are collected at a spinning rate of 6 kHz.